Effect of Arabian Sea-Surface Temperature Anomaly on Indian Summer Monsoon: A Numerical Experiment with the GFDL Model

J. Shukla[1]

Geophysical Fluid Dynamics Program, Princeton University, Princeton, N. J.

ABSTRACT

The global general circulation model of the Geophysical Fluid Dynamics Laboratory has been integrated with and without a cold sea surface temperature (SST) anomaly over the Somali coast and the western Arabian Sea. The temperature anomaly is $-3°C$ near the Somali coast and linearly decreases eastward having zero anomaly at about 1500 km east of the coast. Comparison of the mean of the two model states indicates that the rainfall over India and the adjoining region is drastically reduced due to the colder SST anomaly over the western Arabian Sea. The other associated features due to the cold anomaly are an increase in sea surface pressure over the Arabian Sea, a decrease in local evaporation, and a reduction in the cross equatorial component of the wind at the surface and hence a reduction in the cross equatorial moisture flux. Statistical analysis of the results has been done by comparing the difference between the two mean states ("signal") and the standard deviation of the errors ("noise") in estimating the mean due to the finiteness of the averaging period. It is found that the results of the present numerical experiment are statistically significant.

1. Introduction

It is generally believed that although the onset and the existence of the Asiatic summer monsoon is primarily due to land-sea contrast, the fluctuations and variability of the monsoon activity may depend, at least partially, on the air-sea interaction which takes place during the travel of the monsoon current over the Indian Ocean, Arabian Sea and Bay of Bengal. It has been postulated in earlier studies (viz. Saha, 1970a, 1974; Ellis, 1952) that the sea surface temperature (SST) over the Arabian Sea may have important influences on the monsoon flow and associated rainfall. It is proposed to test such hypotheses using the GFDL general circulation model which seems to have achieved remarkable success in simulating the important features of the global circulation (Manabe *et al.*, 1974). The general circulation model has been integrated first with prescribed mean monthly SST obtained from the U. S. Navy's Hydrographic Office (1964). Then colder SST anomaly is imposed over the western Arabian Sea and the model is again integrated for 48 days. The results of integration for both the experiments are discussed in Section 5.

It may, however, be stated at the outset that the purpose of these experiments is not to claim that the fluctuations in the monsoon are solely caused by SST anomalies over the Arabian Sea (because we simply

do not have adequate past observations to verify such hypotheses), but the main objective is to assess the possible effects, as inferred on the basis of the response of the numerical model. Additional motivation for this study came from the planning of the forthcoming observational experiment called MONEX (Monsoon experiment) so that we may have some basis to decide the areas and extent to which attention should be given during the observational phase of MONEX. It is also hoped that this study would give some insight into the role of the SST in making medium- and long-range numerical weather predictions for the monsoon region.

2. Air-sea interaction over the Arabian Sea

Fig. 1 gives a schematic diagram showing the interaction between the atmospheric and oceanic circulations and their effects on the evaporation, cross-equatorial moisture flux and rainfall over the Indian region, etc. It is well known that during the summer monsoon season strong northward airflow takes place near the eastern coast of Africa and the western Indian Ocean (Findlater, 1969). The wind speed is generally 15 m s^{-1} but may reach as high as 25–45 m s^{-1} on some occasions and the strongest winds are usually found at about 1.5 km above sea level. This wind maximum is usually referred to as the "Somali jet." It is also well known that during the same period a fast northward moving ocean current is located along the east African coast.

[1] Visiting student from the Department of Meteorology, Massachusetts Institute of Technology.
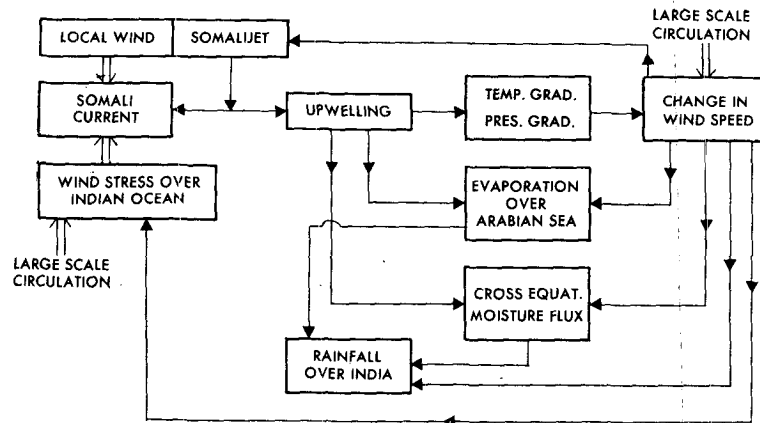
FIG. 1. Schematic representation of air-sea interaction over the Arabian Sea.

This ocean current is referred to as the "Somali current." It is not clearly understood whether the Somali current is caused by the effects of local winds (Leetma, 1972) or in response to the monsoon winds over the Indian Ocean (Lighthill, 1969). However, the upwelling associated with the Somali current off the coast of east Africa is well recognized. Stommel and Wooster (1965) have presented some SST data which show that the SST off the Somalia coast may on occasions be as low as 14°C. By tracing the eastward shift with time of the 26°C isotherm along 10 and 15N, Saha (1970a) has shown that the cold water brought to the surface by upwelling spreads over the western Arabian Sea, and during peak months of the monsoon, most of the western Arabian Sea is enclosed by a 26°C SST isotherm. This feature is further confirmed by the studies of Bruce (1968) and Nimbus 2 observations of 1966.

The possible effects of the SST anomaly as postulated by several workers (viz. Saha, 1970a, b, 1974) may be qualitatively described as follows:

1) Warmer SST anomalies and stronger winds may cause higher evaporation and the monsoon current may be more moist and unstable.

TABLE 1. Values of vertical coordinate (σ) and the corresponding standard heights (approximate values) for each of the 11 vertical finite difference levels.

Level	σ	Standard height (km)
1	0.010	30.93
2	0.038	22.21
3	0.065	18.79
4	0.110	15.45
5	0.190	11.98
6	0.315	8.67
7	0.500	5.44
8	0.685	3.06
9	0.835	1.49
10	0.940	0.52
11	0.990	0.08

2) Colder SST anomalies may cause higher surface pressures and less evaporation over the Arabian Sea and this may reduce the cross-equatorial moisture flux and thus reduce the rainfall over India.

3) Higher pressures over the western Arabian Sea and lower pressures over the eastern Indian Ocean may set up east-west circulation cells.

Due to the paucity of observations over the Arabian Sea and the south Indian Ocean it has not been possible to substantiate any of the hypotheses mentioned earlier, using adequate and reliable data. Ellis (1952) compared the observed SST over the north Indian Ocean during June 1920 and June 1933. In 1920 most of India experienced drought and in 1933 many Indian provinces had floods. His conclusion was that during the flood year (i.e., 1933) the SST over the north Indian Ocean was generally warmer than that during the drought year (1920).

3. Numerical model

The model used is the one which has been described by Manabe et al. (1974). Since the model has been documented in several publications in great detail, only a brief mention will be made here of the important features of the model.

It is an eleven-level (Table 1), global, primitive equation model in the sigma system of spherical coordinates which has 7140 grid points at each level and the grid size is approximately 270 km. The finite-difference form is the one proposed by Kurihara and Holloway (1967), and the scheme of radiative heating and cooling is that of Manabe and Strickler (1964) and Manabe and Wetherald (1967). The scheme for subgrid-scale mixing is the one suggested by Smagorinsky (1963). The solar radiation at the top of the atmosphere varies with latitude and time depending upon the declination of the sun and its distance. The sea surface temperature is prescribed and varies at each ocean grid point with time. For the computation of radiative transfer, an

annual mean observed distribution of the clouds is used which varies only with latitude and height, the distribution of water vapor is predicted by the model, an observed distribution of the ozone is used which varies with the season, latitude and height, and the mixing ratio of CO_2 is assumed to have a constant value of 0.456×10^{-3} everywhere.

Convective adjustment (Manabe et al., 1965) is made to avoid the convective instability of the first kind and it is further hypothesized that this simulates the essential effects of convection, i.e., to neutralize the lapse rate, release the heat of consendation and transfer the heat upward. The surface temperature over land is calculated by requiring a balance between the net fluxes of solar and terrestrial radiation and turbulent fluxes of sensible and latent heat. The schemes for computing the hydrology of the ground surface are similar to the one used by Manabe (1969).

The model has been integrated for a period of 1308 days starting with an initial condition which itself was the mean state attained by the long-term integration of a global model which had January insolation and prescribed sea surface temperature as boundary conditions. The first 1.5 model years were integrated on a low horizontal resolution grid (540 km) and the last two model years were integrated with a high resolution grid (270 km).

The period of integration, which we shall be interested for the purpose of present study, is between model days 1261 and 1308. This corresponds to the calendar dates 15 June through 1 August. (A calendar date is assigned to a given model day depending on the declination of the sun.) For the sake of convenience we shall refer to the calendar dates rather than model day numbers.

For the purpose of the present numerical experiment, the colder SST anomaly over the western Arabian Sea was imposed on the model day corresponding to 15 June and all other features of the model were kept identical. The model was integrated for 48 days with the imposed SST anomaly. For brevity we shall refer to the original integration (using seasonally varying climatological means of SST) as the "Standard run" and the integrations with the SST anomaly as the "Anomaly run."

PERFORMANCE OF THE MODEL IN SIMULATING MONSOON

The detailed analysis of the performance of the model in simulating the seasonal variation of the tropical circulation has been presented by Manabe et al. (1974). Figs. 5.2, 5.5, 4.2d of their paper give the mean July streamlines for the surface and the 190 mb level, and the mean rate of precipitation for June, July, August. In spite of the very simplified treatment of convective adjustment, time invariance of cloud cover and other modeling assumptions, the simulation of the mean tropical summer circulation seems to be reasonable.

One of the limitations seems to be an incorrect rate of precipitation in the vicinity of large and steep mountains. It may be reasonable to assume that this may be due to inadequate horizontal resolution near the mountain slopes and large truncation errors due to very steep gradients of the coordinate surfaces.

The computed rate of precipitation in the northern part of India, near the foothills of the Himalayas, is less than the observed rate of precipitation. This is perhaps because the so-called monsoon trough has not been well simulated by the model. In the actual observations at the surface, the monsoon trough lies close to the foothills and produces substantial amounts of rainfall during the monsoon season. However, with the exception of this feature, the simulation of other flow patterns at the lower levels (viz. cross equatorial flow, Somali jet, etc.), flow patterns at the upper levels (viz. easterly jet, large anticyclonic cell over the Himalayan plateau, etc.) and rainfall over most of peninsular India seems to be reasonable; therefore it was considered justifiable to use this model for the proposed numerical experiment.

4. Specification of SST anomaly

In this model the SST for any ocean point is prescribed as

$$T_*(x,y,t) = \bar{T}(x,y) + C_1(x,y) \sin t + C_2(x,y) \cos t + C_3(x,y) \cos 2t,$$

where $\bar{T}$ is a constant mean value and the coefficients C_1, C_2, C_3 are calculated from the analysis of mean monthly values of May, August, November and February. For the anomaly experiment, $\bar{T}$ was changed on the model day corresponding to 15 June. The SST pattern on 15 June for the standard run is shown in Fig. 2a. The anomaly pattern is shown in Fig. 3 and the SST pattern which was input for the anomaly experiment is shown in Fig. 2b (sum of Figs. 2a and 3). Since C_1, C_2, C_3 in the above equation remain the same for the standard and anomaly experiments, during the entire period of integration, the difference between the two SST patterns remains the same, i.e., as given in Fig. 3.

This anomaly pattern has been chosen after examining the patterns of climatological mean isotherms over the western Arabian Sea and the chosen anomaly pattern is hypothesized to reflect the consequences of strong upwelling associated with the Somali current and eastward spreading of the cold water (Saha, 1970a). In light of the fact that Stommel and Wooster (1965) reported very cold temperatures off the Somali coast, the anomaly of the magnitude of 1–3°C does not seem to be unreasonable. Moreover, Bruce (1968) has reported the existence of a large-scale anticyclonic gyre on the eastern flank of the Somali current which may cause translatory motions of cold water over distances up to approximately 800 km. Examination of more than
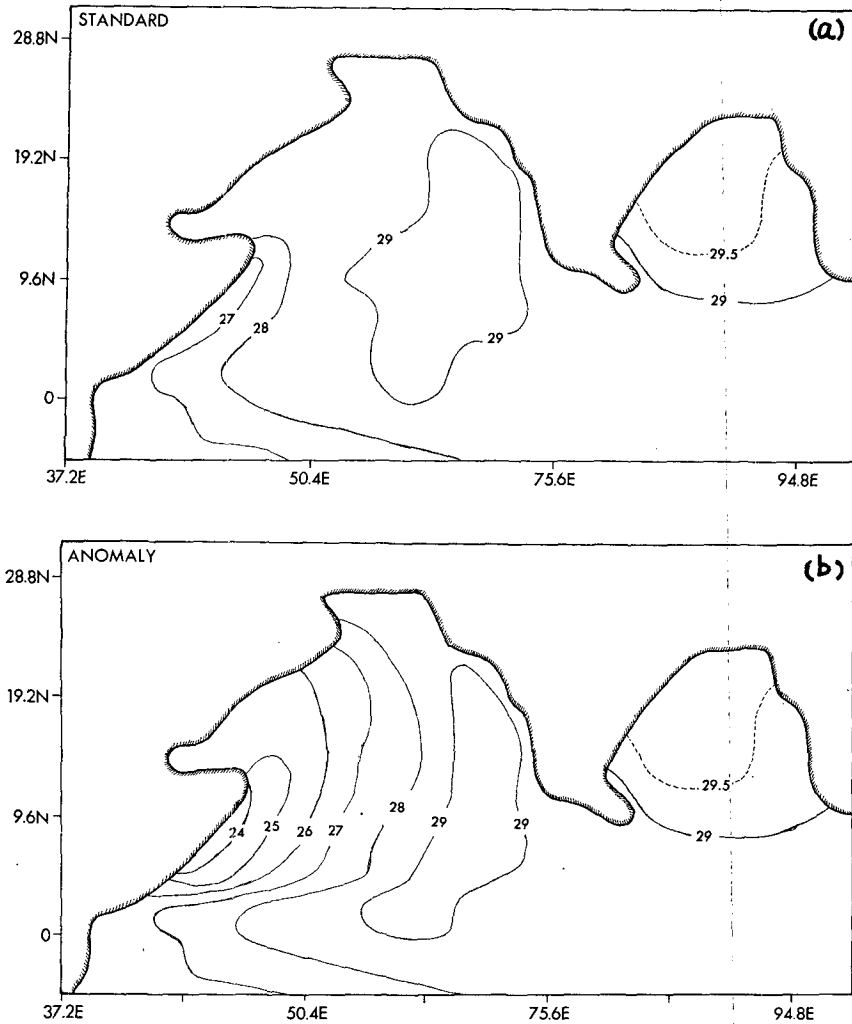
FIG. 2. SST (°C) distribution on model data 15 June for the Standard run (a) and the Anomaly run (b).

20 years of SST data along the ship routes in the western Arabian Sea has further indicated (H. Stommel, personal communication) that the mean monthly anomalies of 2–3°C are not uncommon. The basic idea in the present study is to find the response of such an anomaly on the circulation and rainfall over India. If
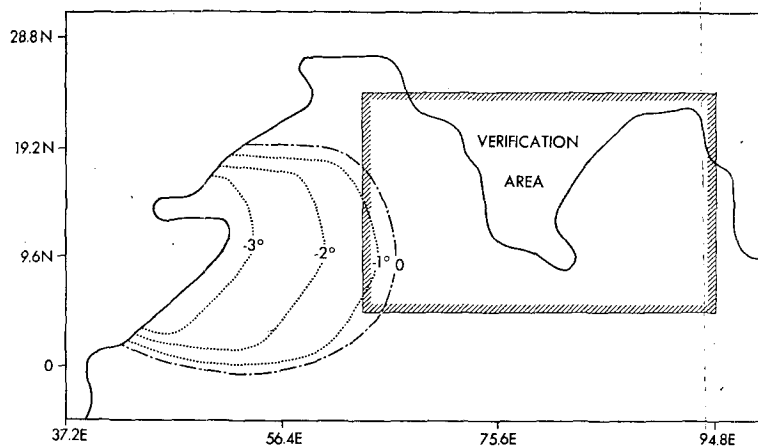

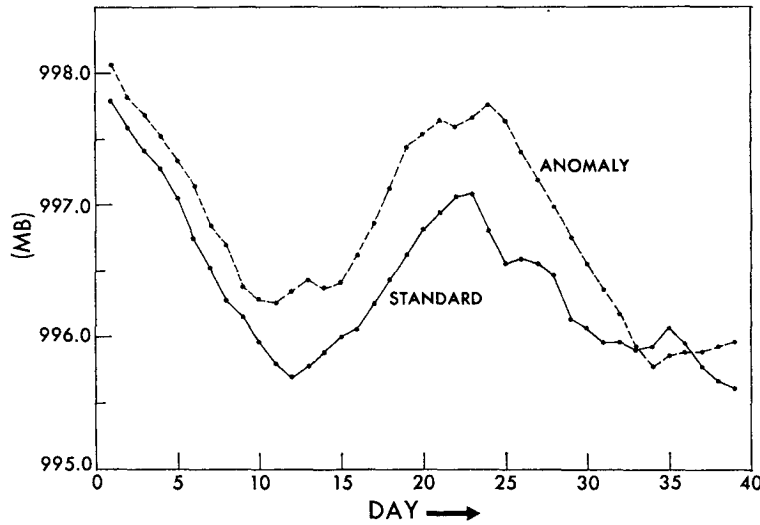FIG. 3. SST (°C) anomaly over western Arabian Sea and location of verification area.

FIG. 4. Surface pressure (mb) averaged over the verification area for the Standard and Anomaly runs.

the response is very significant, we can draw useful information for designing an observational program to find the association between the SST anomalies and rainfall over India and adjoining areas.

Although the SST anomaly was imposed rather abruptly on the model day 15 June, it may not cause any serious effects on the results because the period for which the results are examined is several days after the starting period. It may, however, be interesting to find the effect of a gradually imposed SST anomaly.

5. Results

In this section, we shall present the results of the standard and anomaly runs and discuss the important differences between the two. The basic field in which we are interested is the rate of precipitation and we shall discuss this in detail. However, for the sake of completeness in our discussion we shall also discuss

the differences between the two experiments for the sea-surface pressure, evaporation, and cross-equatorial moisture flux. For the purpose of comparison, special emphasis is given to the area adjoining India. This limited region, as shown in Fig. 3, will be referred to as the verification area.

a. Surface pressure and wind

Fig. 4 gives the 10-day running mean of the daily values of surface pressure average over the verification area for the standard and anomaly runs. It is clearly seen that the surface pressure is higher for the anomaly run. This difference is found to be larger over the region of the anomaly itself. Although the colder SST anomaly is not introduced over the verification area, the direction of the wind flow close to the surface is persistently from the anomaly area toward the verification area. The decrease in temperature and increase in surface pressure
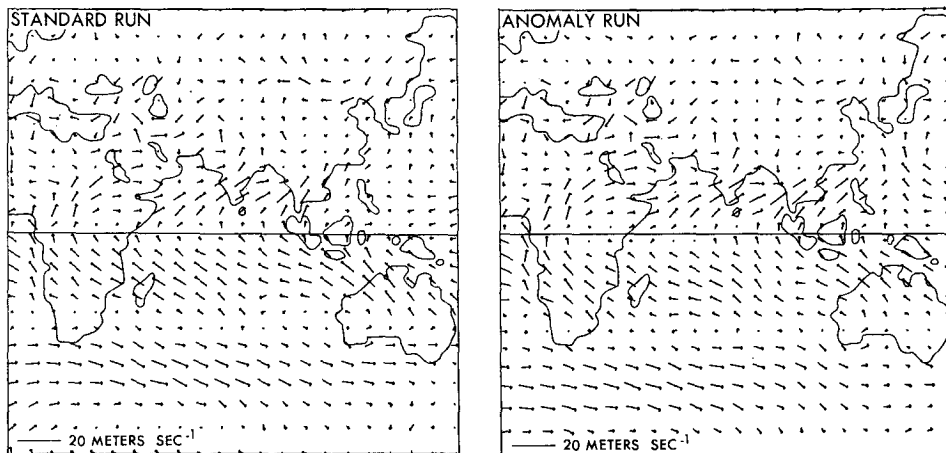

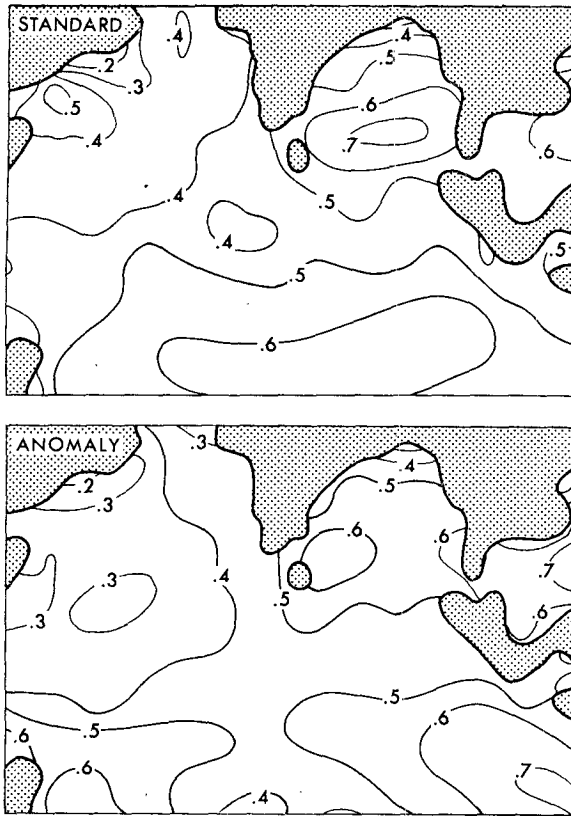FIG. 5. Mean monthly (July) surface wind vectors for Standard and Anomaly runs.

FIG. 6. Mean monthly (July) rate of evaporation (cm day⁻¹) for the Standard and Anomaly runs.

are found to occur concurrently which is hydrostatically consistent. Although the changes in the surface pressure are not large, they have significant effects on the surface flow pattern, especially the cross-equatorial

component of the wind. An increase in the surface pressure over the Arabian Sea may tend to reduce the south-north pressure gradient and hence also the intensity of the meridional wind component across the equator. This is indeed seen in Fig. 5 which shows that the surface winds at the equator are quite weak in the anomaly run compared to the standard run.

b. Evaporation

Fig. 6 gives the mean-monthly (July) rate of evaporation for the anomaly and standard runs. It is natural to expect that the evaporation would be less for colder sea surface temperatures, but we must also note that the reduction in the evaporation as observed in Fig. 6 is not only due to reduced SST but also due to reduced surface wind speed, which is a parameter in determining the rate of evaporation at the surface.

c. Cross-equatorial moisture flux

Fig. 7 shows cross sections of cross-equatorial moisture flux due to mean-monthly (July) meridional wind and mixing ratio for both experiments. This parameter has been chosen for two reasons. First, the cross-equatorial moisture flux has been a matter of considerable interest in previous studies (Saha, loc. cit.), especially in its relation with rainfall over India. Second, this single parameter reflects both the changes in evaporation and wind speed. It is seen from Fig. 7 that the cross-equatorial moisture flux is substantially reduced in the anomaly experiment compared to the standard experiment, especially between 50–90E. Since the cross-equatorial flux has decreased considerably, it has given rise to flux convergence south of the anomaly region and hence enhancement of rainfall there.
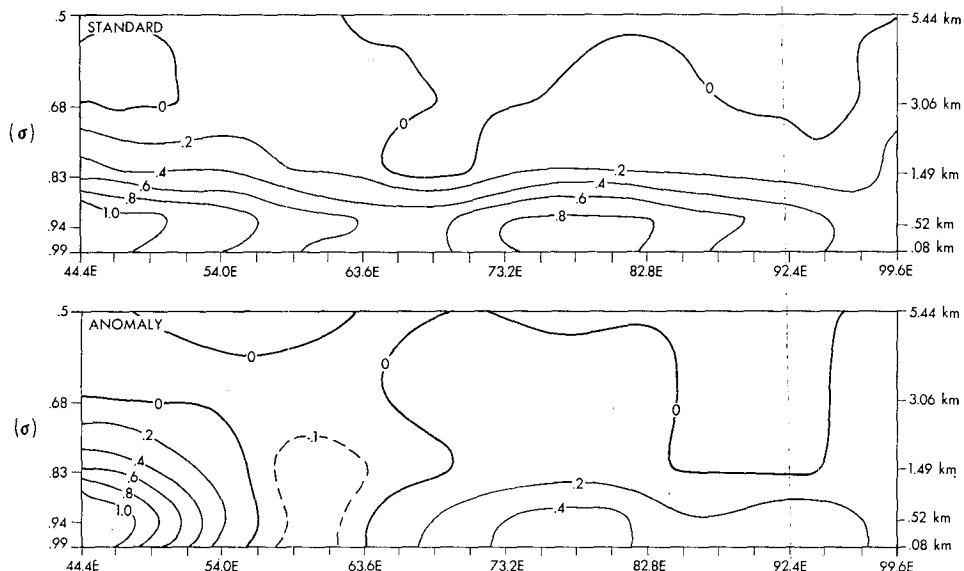

FIG. 7. Cross equatorial moisture flux (10 cm s⁻¹) due to mean monthly (July) meridional wind and mixing ratio.
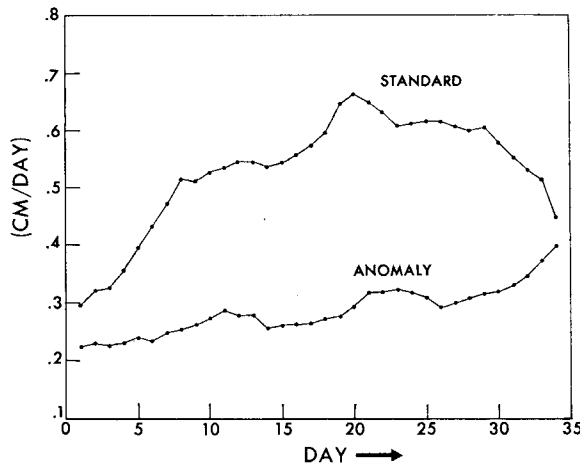
FIG. 8. Rate of precipitation (cm day⁻¹) averaged over the verification area for the Standard and Anomaly runs.

This may partly explain the reduction of rainfall over the verification area.

d. Rate of precipitation

Fig. 8 gives the 15-day running mean of the daily values of rate of precipitation (averaged over the verification area) for both experiments. The rate of precipitation in the anomaly run is quite small compared to the standard run. This result supports the hypothesis, mentioned before, that colder SST anomalies in the western Arabian Sea and along the Somali coast may tend to reduce the monsoon rainfall over India and adjoining areas. Detailed statistical analysis, however, must be done to ensure that these changes are indeed significant. The results of such analysis are given in the next section.

The differences between the anomaly and standard runs tend to decrease after 30 days. This may be due to certain feedback mechanisms which may be present in the model dynamics. At this stage, we do not have a definite explanation for this.

6. Statistical analysis of the results

It has been pointed out by Leith (1973) that in numerical experimentation studies in which we are interested in detecting the influence of external changes, such as in sea surface temperature or solar constant, we must be able to distinguish between the "signal," i.e., the change in the two climatic means, and the "noise," i.e., the natural fluctuation in finite-time mean state. To be able to claim that the differences between the two experiments are genuine and significant, we must take the average over longer periods and this averaging period should be decided on the basis of analysis of variance of the time series of variables describing the model states. It may be mentioned that several papers, describing the response of general

circulation models to SST anomalies, have recently appeared (Houghton et al., 1974; Spar, 1973; Rowntree, 1972), but they have confined their discussion only to the description of the differences between the standard and control runs and there is no attempt to determine if those differences are statistically significant. This seems to be a serious limitation of these studies because for reliable interpretation of the results of such numerical experiments, the random fluctuations must be distinguished from the genuine changes.

Following Leith (loc. cit.), for a random time series $\psi(t)$ with mean μ and standard deviation σ, the error $\bar{\phi}(t)$ in estimating the mean due to averaging over a limited period T is given by

$$\bar{\psi}(t) = \mu + \bar{\phi}(t),$$

where

$$\overline{(\ )} = \frac{1}{T} \int_{-T/2}^{T/2} (\ )dt, \quad \psi(t) = \mu + \phi(t).$$

Here

$$\langle \phi(t) \rangle = 0, \quad \langle \phi(t)\phi(t+\tau) \rangle = \sigma^2 R(\tau),$$

where $\langle\ \rangle$ denotes the ensemble average and $R(\tau)$ is the correlation at lag time τ. The variance of $\bar{\phi}(t)$ may be given as

$$\langle \bar{\phi}(t)\bar{\phi}(t) \rangle = \sigma_T^2 = \frac{2\sigma^2}{T} \int_0^T \left(1 - \frac{\tau}{T}\right) R(\tau)d\tau. \quad (1)$$

In Leith's analysis σ_T is referred to as noise and the difference between the means of the two model states, i.e., $\Delta\mu [= \mu_2 - \mu_1]$, is referred to as signal. For a result to be significant the signal-to-noise ratio must be greater than 1.

Since we were primarily interested in the changes in the rate of precipitation over the verification area, such detailed statistical analysis will be presented only for this parameter. Fig. 9 gives the variation of σ_T for various values of T and it is reasonable to expect that the value of σ_T decreases as we increase the averaging period. $\Delta\mu$ for $T = 48$ days has also been shown in Fig. 9 and it is seen that for any averaging period greater than 8 days, the signal-to-noise ratio is larger than 1. This is of course due to the fact that the changes
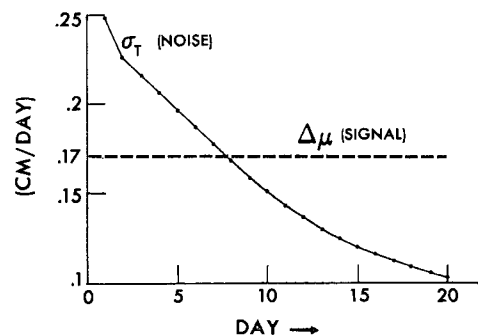

FIG. 9. Values of σ_T as a function of averaging period for rate of precipitation (cm day⁻¹) over the verification area.
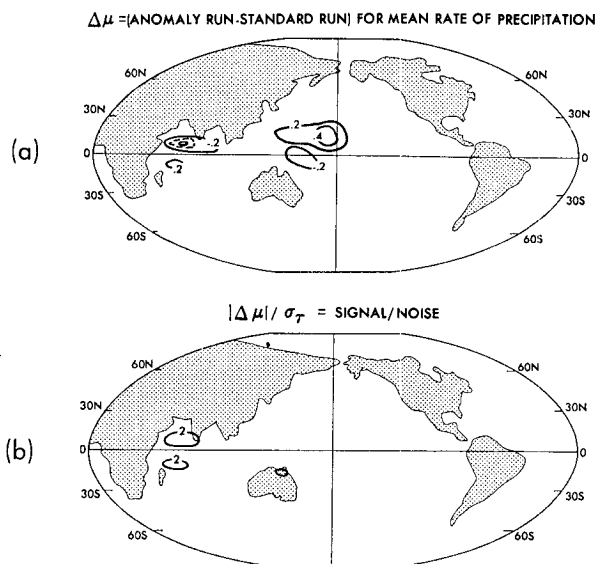
Δμ =(ANOMALY RUN-STANDARD RUN) FOR MEAN RATE OF PRECIPITATION

(a)

|Δμ|/σ$_T$ = SIGNAL/NOISE

(b)

FIG. 10. Global distribution of signal Δμ (cm day^{-1})
and the signal-to-noise ratio Δμ/σ$_T$.

in the mean are rather large. The corresponding period for the surface pressure field was found to be nearly 20–25 days.

Since the model used is global we have the values of rate of precipitation for the whole globe. Subtracting the standard run values from the anomaly run values we may obtain the difference map. Such a difference map for the mean rate of precipitation is given in Fig. 10a. But we must now make the aforementioned statistical analysis to see which of these changes are really significant. To make this test, the signal-to-noise ratio was computed for the individual grid points. Before making such computations the original field was smoothed by replacing each grid point value by the average of all the values within a three grid length distance from that point. This smoothing was done to reduce the small-scale spatial variability of rainfall at different grid points. The result of the signal-to-noise ratio computation is shown in Fig. 10b. It is clearly seen that although the differences between the standard and anomaly runs were quite large in the Pacific they turned out to be not significant because the changes in the mean were not appreciably larger than the standard deviation of the "random" fluctuations. The changes that are significant are mostly found in the vicinity of the temperature anomaly.

7. Concluding remarks

The results of this numerical experiment tend to suggest that colder SST anomalies over the western Arabian Sea and Somali coast may cause reduction in the monsoon rainfall over India and adjoining areas. The features associated with the cold SST anomaly seem to be an increase in the surface pressure, a decrease in the rate of evaporation, and a reduction in the

cross-equatorial wind and hence a reduction in the cross-equatorial moisture flux over the anomaly region and adjoining areas. Decrease in the rainfall north of the equator is also accompanied by increase in the moisture flux convergence and rainfall south of the equator. The statistical analysis given in Section 6 shows that the results are indeed significant.

However, while interpreting these results, the limitations of this study should also be kept in mind. Besides the shortcomings of the numerical model in simulating the general circulation of the atmosphere, the most serious limitation of the study is that the model used here is not designed to simulate an interacting ocean-atmosphere system. SST is used only as the boundary condition and is prespecified. The region under consideration is one which has very strong interaction between the atmosphere and ocean. It is not clear what feedback mechanisms may exist to change the wind circulation and SST anomaly. Second, the statistical analysis suffers from the limitation that it does not take into account the plausibility of a significant change in the mean state due to even a random perturbation in the initial state or boundary condition. This question may be partially settled by repeating the numerical experiment with a random anomaly in SST, but this could not be done due to large computer time requirements for this purpose.[2]

Although the results of this experiment suggest a clear influence of SST anomalies in the Arabian sea on the monsoon rainfall, it is not implied that this is the only important factor affecting the summer monsoon activity because we recognize that cyclogenesis over the Bay of Bengal and other large-scale features are quite important in controlling the fluctuations in the moonsoon activity. Since the Arabian Sea is a relatively cloud-free region, it is hoped that direct measurements of SST from the satellites would provide adequate data over a long period to verify such hypotheses.

[2] 100 hours of CPU time of IBM 360/195 for each experiment.

REFERENCES

Bruce, J. G., 1968: Comparison of near surface dynamic topography during the two monsoons in the western Indian Ocean. *Deep Sea Res.*, 15, 665–677.

Ellis, R. S., 1952: A preliminary study of a relation between surface temperature of the north Indian Ocean and precipitation over India. M.S. thesis, Dept. of Meteorology, Florida State University.

Findlater, J., 1969: Interhemispheric transport of air in the lower troposphere over the western Indian Ocean. *Quart. J. Roy. Meteor. Soc.*, **95**, 400–403.

Houghton, D. D., J. E. Kutzbach, M. McClintock and D. Suchman, 1974: Response of a general circulation model to a sea temperature perturbation. *J. Atmos. Sci.*, **31**, 857–868.

Kurihara, Y., and J. L. Holloway, 1967: Numerical integration of a nine-level global primitive equation model formulated by the box method. *Mon. Wea. Rev.*, **95**, 509–530.

Leetma, A., 1972: The response of the Somali current to the Southwest monsoon of 1970. *Deep Sea Res.*, **19**, 319–325.

Leith, C., 1973: The standard error of time-average estimates of climatic means. *J. Appl. Meteor.*, **12**, 1066–1069.

Lighthill, M. J., 1969: Dynamic response of the Indian Ocean to onset of the southwest monsoon. *Phil. Trans. Roy. Soc. London*, **A265**, 45–92.

Manabe, S., 1969: Climate and ocean circulation, Part 1: The atmospheric circulation and hydrology of the earth's surface. *Mon. Wea. Rev.*, **97**, 739–774.

——, and R. F. Strickler, 1964: On the thermal equilibrium of the atmosphere with convective adjustments. *J. Atmos. Sci.*, **21**, 361–385.

——, and R. T. Wetherald, 1967: Thermal equilibrium of the atmosphere with a given distribution of relative humidity. *J. Atmos. Sci.*, **24**, 241–259.

——, J. Smagorinsky and R. F. Strickler, 1965: Simulated climatology of a general circulation model with a hydrologic cycle. *Mon. Wea. Rev.*, **93**, 709–798.

——, D. G. Hahn, and J. L. Holloway, 1974: The seasonal variation of the tropical circulation as simulated by a global model of the atmosphere. *J. Atmos. Sci.*, **31**, 43–83.

Rowntree, P. R., 1973: The influence of tropical east Pacific Ocean temperature on the atmosphere. *Quart. J. Roy. Meteor. Soc.*, **98**, 290–321.

Saha, K. R., 1970a: Zonal anomaly of sea surface temperature in equatorial Indian Ocean and its possible effect upon monsoon circulation. *Tellus*, **22**, 403–409.

——, 1970b: Air and water vapor transport across the equator in western Indian Ocean during northern summer. *Tellus*, **22**, 681–687.

——, 1974: Some aspects of the Arabian sea summer monsoon. *Tellus*, **26**, 464–476.

Smagorinsky, J., 1963: General circulation experiments with primitive equations, 1. The basic experiment. *Mon. Wea. Rev.*, **93**, 99–164.

Spar, J., 1973: Some effects of surface anomalies in a global general circulation model. *Mon. Wea. Rev.*, **101**, 91–100.

Stommel, H., and W. S. Wooster, 1965: Reconnaissance of the Somali current during the southwest monsoon. *Proc. Nat. Acad. Sci. U. S.*, **54**, 8–13.